Conductive Graphene Fibers for Wire-Shaped Supercapacitors Strengthened by Unfunctionalized Few-Walled Carbon Nanotubes

Yanwen Ma,[†,‡] Pan Li,[†] Jennifer W. Sedloff,[†] Xiao Zhang,[†] Hongbo Zhang,[†] and Jie Liu*[,†]

[†]Department of Chemistry, Duke University, Durham, North Carolina 27708, United States and [‡]Key Laboratory for Organic Electronics & Information Displays and Institute of Advanced Materials, Nanjing University of Posts & Telecommunications, Nanjing 210046, China

ABSTRACT Graphene fibers are a promising electrode material for wire-shaped supercapacitors (WSSs) that can be woven into textiles for future wearable electronics. However, the main concern is their high linear resistance, which could be effectively decreased by the addition of highly conductive carbon nanotubes (CNTs). During the incorporation process, CNTs are typically preoxidized by acids or dispersed by surfactants, which deteriorates their electrical and mechanical properties. Herein, unfunctionalized few-walled carbon nanotubes (FWNTs) were directly dispersed in graphene oxide (GO) without preoxidation or surfactants, allowing them to maintain their high conductivity and perfect structure, and then used to prepare CNT-reduced GO (RGO) composite fibers by wet-spinning followed by reduction. The pristine FWNTs increased the stress strength of the parent RGO fibers from 193.3 to 385.7 MPa and conductivity from 53.3 to 210.7 S cm^{-1}. The wire-shaped supercapacitors (WSSs) assembled based on these CNT-RGO fibers presented a high volumetric capacitance of 38.8 F cm^{-3} and energy density of 3.4 mWh cm^{-3}. More importantly, the performance of WSSs was revealed to decrease with increasing length due to increased resistance, revealing a key issue for graphene-based electrodes in WSSs.

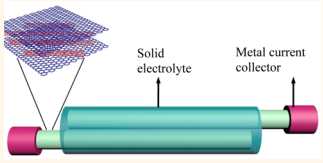

KEYWORDS: graphene · carbon nanotubes · fibers · solution spinning · wire · supercapacitors

Increasing interest in wearable electronics requires the development of compatible energy storage devices such as wire-shaped supercapacitors (WSSs) that can be woven into clothes.[1,2] The most critical requirement for supercapacitors to be used in wearable electronics is changing their electrodes from a film to a wire or fiber configuration. Among all electrode materials, carbon nanotubes (CNTs) and graphene are the most desirable candidates for this application not only because of their remarkable electrical, mechanical, and thermal properties and large specific surface areas, but also because they can be spun into fibers that directly act as WSS electrodes.[3−16] Compared with the preparation of CNT fibers, which typically involves solid-state spinning or super acid solution spinning,[17−19] the process to fabricate graphene oxide (GO) fibers by wet-spinning is easier, milder, and less costly.[20−22] However, the conductivity of reduced GO (RGO) fibers ranges only from 10 to 400 S/cm,[7,20−22] far below that of CNT fibers (500−5000 S/cm),[17−19,23] which presents a major bottleneck for their application in WSSs.

According to the previous studies on RGO-based films and fibers,[14,15,24−26] a general strategy to improve their conductivity is incorporating highly conductive CNTs during their manufacture to generate desirable synergistic effects. For example, the recent work on continuous preparation of RGO fibers by a hydrothermal process applied this strategy to improve the fibers' conductivity from 12 to 102 S cm^{-1} after acid-oxidized single-walled CNTs (SWNTs) were added to RGO in a 1:1 weight ratio.[15] However, the tensile strength decreased 50% after the addition of oxidized CNTs, likely due to an increased amount of defects in the CNTs, which would weaken their van der Waals interactions with the RGO sheets.[15] Pristine SWNTs were effectively used to reinforce RGO fibers mechanically using high-content (3:1 weight ratio of surfactant to SWNTs) sodium dodecyl benzenesulfonate.[27] However, it is believed that the surfactant was

* Address correspondence to j.liu@duke.edu.

Received for review September 23, 2014 and accepted January 27, 2015.

Published online January 27, 2015
10.1021/nn505412v

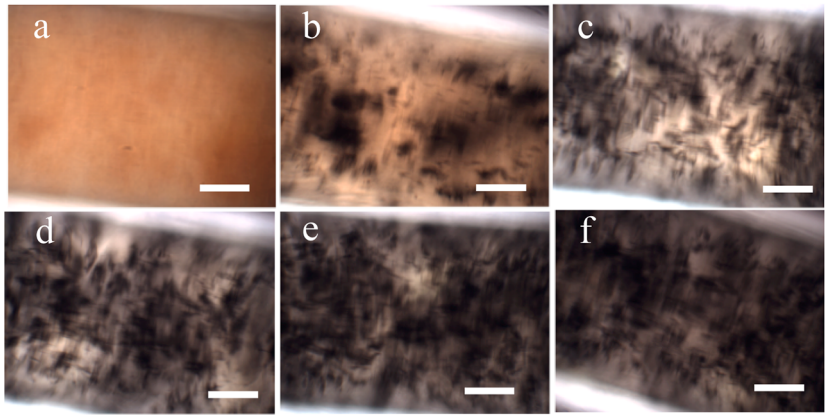

Figure 1. Optical micrographs of GO (a) and CNT-GO aqueous solutions with FWNT/GO mass ratio of 1:8 (b), 1:6 (c), 1:4 (d), 1:3 (e) and 1:2 (f). Scale bars: 100 μm.

detrimental to the electrical conductivity of the resulting fibers. Interestingly, GO sheets themselves, containing aromatic regions and hydrophilic oxygen groups, could behave like an amphiphilic molecule, and thus can act as a dispersant to suspend pristine CNTs in water.[28,29] This interaction between GO and unfunctionalized CNTs allows for the possibility to prepare composite fibers by wet-spinning as long as the mixed GO−CNT solution maintains a liquid crystalline state, the prerequisite for wet spinning.

Here, making use of the excellent dispersion capability of GO, pristine few-walled CNTs (FWNTs) were dispersed into GO suspension and spun into composite fibers. In previous approaches, the use of oxidized-CNTs as additives deteriorated the mechanical properties of the resultant fibers.[15] In contrast, use of highly π-conjugated unfunctionalized FWNTs as an additive in RGO fibers enables simultaneous increase of the ductility, strength and flexibility of the fibers. The presence of pristine FWNTs significantly enhances the conductivity of the composite fibers up to 210.7 S cm^{-1}. Flexible two-ply WSSs were assembled from the as-prepared composite fibers, showing a high volume capacitance (38.8 F cm^{-3}), good charge/discharge performance, and high energy density (3.4 mWh cm^{-3}). In addition, the deleterious effect of increased electrode length on device performance was revealed due to increased resistance, and then a possible route was provided to resolve this issue by plying many fibers together in each electrode.

RESULTS AND DISCUSSION

GO sheets with sizes of tens of micrometers (Figure S1 in Supporting Information) were synthesized from expanded graphite following a previously reported method.[21] Here FWNTs were applied as reinforcing filler based on their remarkable electric conductivity and near perfect graphitization structures. They tend to be easier separated and dispersed than single-walled CNTs as well as have better conductivity and mechanical strength compared with multiwalled CNTs.[30] Unfunctionalized FWNTs with CNT/GO mass ratio between 1:8 and 1:2 can be readily dispersed by GO nanosheets in aqueous solution. The optical micrographs in Figure 1 show the mixed state of FWNTs and GO in the solution, where the GO matrix is a homogeneous brown color and the CNTs are black. The majority of CNTs are separated by GO sheets, but some small bundles exist because of the strong interactions between pristine FWNTs. At CNT mass fractions of 50% or greater, the CNT bundles became large and visible to the naked eye. The presence of many CNT bundles decreases the stability of the solutions by interfering with the electrostatic repulsion between oxygen-containing groups on GO sheets, eventually resulting in the coagulation of GO platelets. For all the well-dispersed CNT-GO composite solutions shown in Figure 1, nematic liquid crystal features were observed in polarized optical microscopy (Figure S2 in Supporting Information), suggesting suitability for wet spinning.

GO and CNT-GO composite fibers with CNT/GO mass ratios between 1:8 and 1:2 were fabricated by Petridish wet-spinning approach (Figure S3 in Supporting Information). However, continuous fibers could not be obtained from solutions with mass fraction of CNTs being 50% or greater, since the amount of unfunctionalized FWNTs was beyond the dispersion capability of GO, as discussed above. The as-spun GO and CNT-GO composite fibers were then reduced in hydroiodic acid aqueous solution to produce the corresponding RGO and CNT-RGO composite fibers. Figure 2 shows scanning electron microscope (SEM) images of the reduced fibers, with diameters ranging from 20 to 25 μm. The RGO sheets within the fibers oriented along their axes and stacked together tightly. The incorporated CNTs in the fibers were pressed by RGO sheets as shown in the cross-section of these composite fibers. Notably, the CNTs were also partially aligned along the axial direction, especially in fibers with CNT/GO ratios lower than 1:3. It is beleived that the presence of GO induces CNT

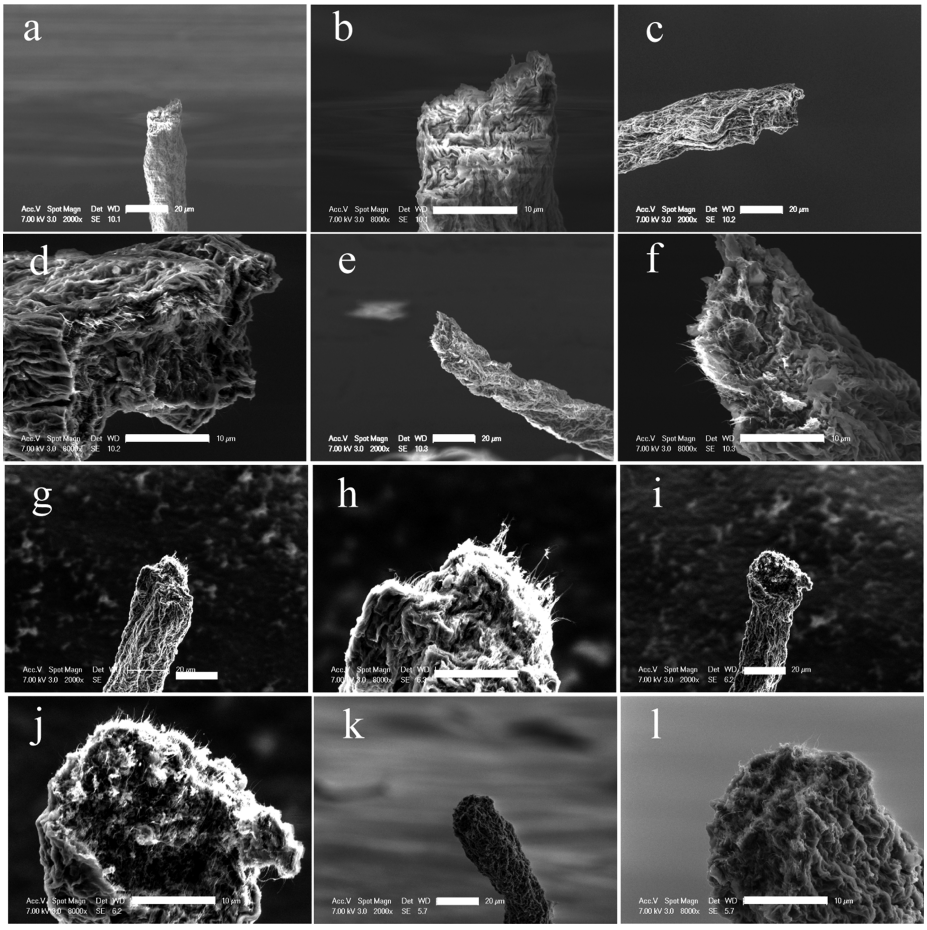

Figure 2. Typical SEM images of RGO and CNT-RGO fibers. (a, b) RGO; (c, d) CNT_1-RGO_8; (e, f) CNT_1-RGO_6; (g, h) CNT_1-RGO_4; (i, j) CNT_1-RGO_3; (k, l) CNT_1-RGO_2. Scale bars: 20 μm (a, c, e, g, i, k), 10 μm (b, d, f, h, j, l).

TABLE 1. Physical, Mechanical, and Electrical Properties of RGO and CNT-RGO Fibers

fiber	diameter (μm)	density (g cm^{-3})	modulus (GPa)	strength (MPa)	strain (%)	conductivity (S cm^{-1})
RGO	20 ± 1	0.81 ± 0.01	19.1 ± 1.5	193.3 ± 6.4	1.6 ± 0.1	53.5
CNT_1-RGO_8	24 ± 2	0.94 ± 0.02	10.5 ± 2.1	232.2 ± 11.3	2.9 ± 0.3	89.2
CNT_1-RGO_6	22 ± 3	1.01 ± 0.03	6.2 ± 0.5	278.4 ± 10.5	6.8 ± 0.5	138.6
CNT_1-RGO_4	24 ± 2	1.08 ± 0.03	5.3 ± 0.5	385.7 ± 17.5	11.4 ± 0.9	210.7
CNT_1-RGO_3	22 ± 1	1.11 ± 0.02	4.2 ± 0.3	218.1 ± 15.1	5.6 ± 0.1	275.1
CNT_1-RGO_2	20 ± 3	–	4.6 ± 0.4	149.4 ± 12.6	4.1 ± 0.2	161.0

alignment during solution spinning. As a result, a high GO fraction was beneficial for CNT alignment. We also deduce that these partially aligned CNTs experienced stretching force during the spinning process and shrinkage while solidifying. This phenomenon were reflected by the corrugations existing along the composite fiber axis (Figure S4 in Supporting Information). Intuitively, the corrugated CNT-RGO composite fibers were more flexible and elastic than the neat RGO fibers.

Stress–strain curves of the prepared fibers were measured (Figure S4 in Supporting Information) and the calculated mechanical properties are listed in Table 1. Compared with GO-based fibers (Table S1 in Supportinging Information), the reduced ones had enhanced strength and elongation, similar to previous results.[27] The tensile strength and Young's modulus of the parent RGO fiber were ~193.3 MPa and ~19.1 GPa respectively, comparable to those of previously reported RGO-based fibers.[7,20−22] The mechanical properties of CNT-RGO composite fibers were found to be very sensitive to the CNT mass fraction. The tensile strength and strain initially increased and then decreased when the ratio of CNT to GO increased. CNT_1-RGO_4 fiber had the largest elongation, ~11.4%, and the highest tensile strength, ~385.7 MPa. The significantly enhanced ductility likely results from the corrugated structure observed in SEM images (Figure S4 in Supporting Information). The improvement on strength and flexibility by addition of CNTs can be explained as a synergistic effect generated from the interconnection

of RGO sheets and partially aligned CNTs.[27] For neat CNT fibers, high-quality CNTs with minimal defects are necessary for strong fibers.[18] Similarly, the unfunctionalized FWNTs with fewer defects than functionalized FWNTs were helpful in this case, leading to stronger van der Waals forces between FWNTs and RGO sheets and thus increasing the tensile strength. However, overloading of CNT fillers unavoidably produces voids in the RGO matrix due to the increased presence CNT bundles, and leading to deterioration of mechanical properties of the whole fiber. This is the main reason why the tensile strength and strain of composite fibers decreased when the proportion of CNTs was increased to values above 25 wt %. The moduli of composite fibers decreased monotonically with increasing CNT content, similar to the change in moduli observed in SWNT/RGO/PVA composite fibers.[27] Besides the mechanical improvement, an appropriate amount of CNTs also increased fiber conductivity. For example, the conductivity of the CNT_1-RGO_4 fiber was 210.7 S m^{-1}, which is over three times higher than that of the RGO fibers (53.5 S m^{-1}) and much better than fibers using oxidized SWNTs as the additive.[15] It is also seen that the conductivity did not always increase with increasing CNT proportion. The CNT_1-RGO_3 fiber had the highest conductivity of 275.1 S m^{-1}, while the CNT_1-RGO_2 fiber had a much lower conductivity of 161.0 S m^{-1}. From the preceding characterization and analysis, it is reasonable to deduce that the lowered conductivity of the CNT_1-RGO_2 fiber is caused by the weakened alignment of these two carbon nanomaterials and the possible existence of voids in the fiber.

All-solid-state two-ply fiber supercapacitors were assembled by using PVA-H_3PO_4 gel as a solid electrolyte. Here CNT_1-RGO_4 fibers were used as representative electrodes based on their combination of good

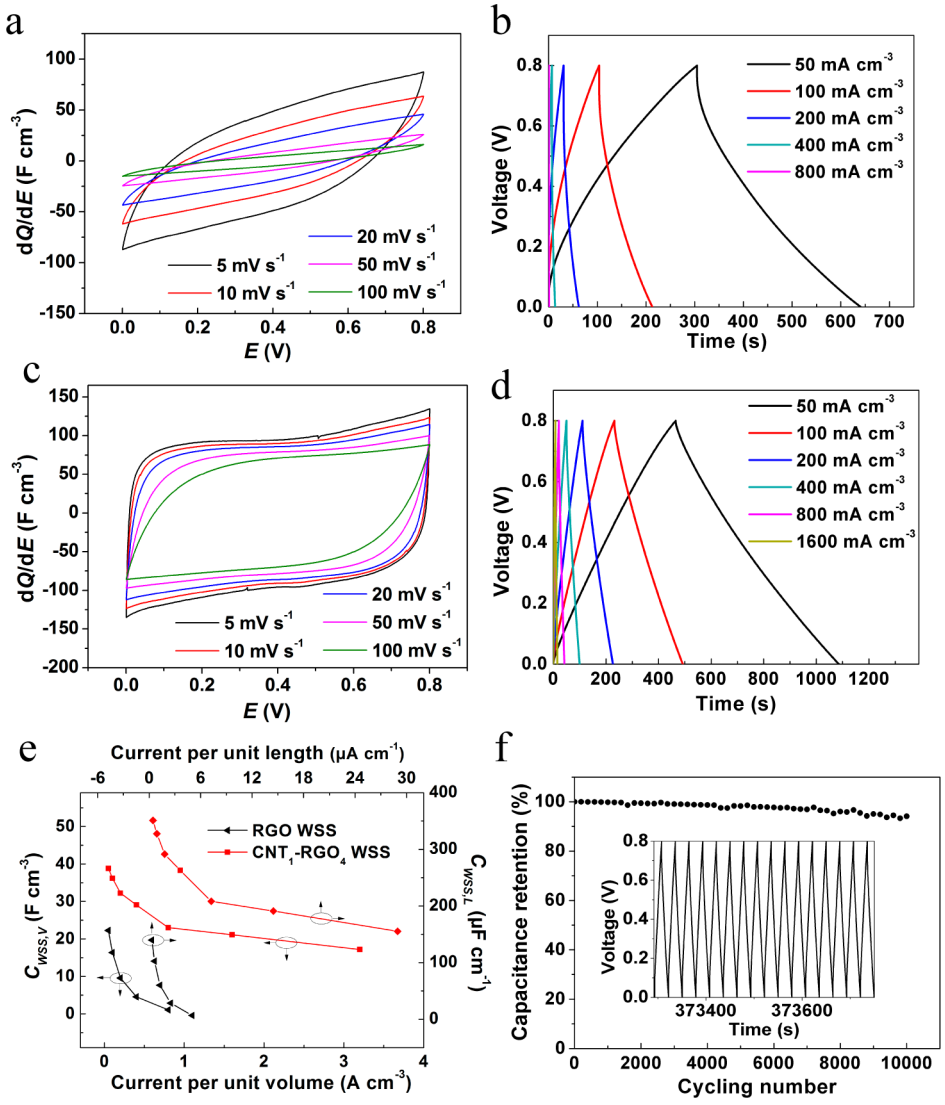

Figure 3. Electrochemical performance of two-ply WSSs. (a) CV curves and (b) galvanostatic charge/discharge curves of RGO device; (c) CV curves and (d) galvanostatic charge/discharge curves of CNT_1-RGO_4 devices; (e) Specific capacitance at different discharging current densities; (f) Capacitance retention *versus* cycle number at 800 mA cm^{-3}. The inset in (f) displays galvanostatic charge−discharge curves over 6000 cycles.

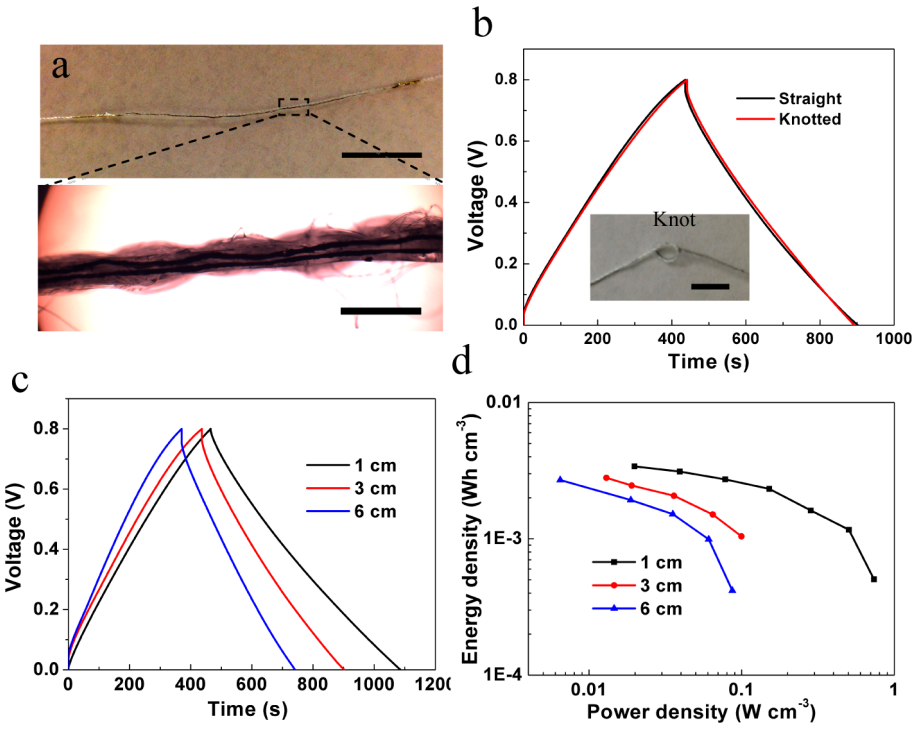

Figure 4. (a) Photograph (upper) and micrograph (bottom) of a 3 cm CNT_1-RGO_4 WSS integrated onto a polyester yarn; (b) Galvanostatic charge−discharge curves of the 3 cm WSS on polyester yarn before and after knotted at current density of ~50 mA cm^{-3}; (c) Charge−discharge curves of 1, 3, and 6 cm CNT_1-RGO_4 WSSs at current density of ~50 mA cm^{-3}; (d) Volumetric energy and power densities for CNT_1-RGO_4 WSS with device length of 1, 3, and 6 cm. Scale bars: 1 cm (a), 100 μm (b), 0.5 cm (c).

mechanical property and electrochemical performance in three-electrode tests (SI 6 in Supporting Information). The effective length of the device was controlled to be 1 cm and the effective volume was around ~1.0×10^{-5} cm^3. For comparison, a neat RGO fiber WSS was also prepared using the same approach. The CV curves of the RGO fiber WSS in Figure 3a are spindle shaped, especially at scan rates higher than 10 mV s^{-1}, indicating the poor resistance behavior of the device. Correspondingly, the galvanostatic charge/discharge curves (Figure 3b) are not in symmetric triangular shapes and have large voltage drops at the beginning of the discharge process, suggesting that the device is not an ideal supercapacitor and its performance is heavily weakened by the large resistance of the electrodes. In contrast, for the CNT_1-RGO_4 fiber WSS, the CV curves (Figure 3c) are almost rectangular and maintain their shape even at a high scan rate of 100 mV s^{-1}. The charge/discharge curves (Figure 3d) show near-linear symmetric shapes, indicating good charge propagation in the electrodes. The capacitances of the WSSs at different charge/discharge current density are given in Figure 3e. Clearly, the CNT_1-RGO_4 fiber device had much higher capacitance and better rate performance than the RGO fiber device. For the CNT_1-RGO_4 fiber WSS, the length capacitance ($C_{WSS,L}$) is 351 μF cm^{-1}, corresponding to a volumetric capacitance ($C_{WSS,V}$) of 38.8 F cm^{-3} at 50 mA cm^{-3} (Figure 4e). Its $C_{WSS,V}$ was maintained at 50% when the discharging current density increased by a factor of 30 from 50 to 1600 mA cm^{-3}, indicating its good charge/discharge performance. Especially, its power density can reach 0.5 W cm^{-3} at an energy density of 1 mWh cm^{-3}, much better than some previously reported WSSs.[7,31] The improved power is attributed to the highly increased conductivity, which is exceptionally important for wearable applications, where some garments may take hundreds of feet of energy storing yarns to fabricate a full device. The long-term cycling stability was evaluated using the galvanostatic charge/discharge technique conducted at 800 mA cm^{-3} (Figure 3f). The device shows a capacitance retention of above 93% over 10 000 cycles, revealing its outstanding electrochemical stability.

To further examine the flexibility of CNT_1-RGO_4 WSSs, a 3 cm device was intergrated with a polyster yarn (~100 μm) by using the PVA-H_3PO_4 gel electrolyte as an adhesive (Figure 4a). The polyster yarn protected the WSS well during stretching and bending. Even while knotted, the device retained its original performance, as reflected by the galvanostatic charge/discharge curves in Figure 4b. In addition, an interesting result is that its $C_{WSS,V}$ (30.6 F cm^{-3}, Figure S7a in Supporting Information) at 50 mA cm^{-3} is smaller than that of the 1 cm device. When device length was extended to 6 cm, the $C_{WSS,V}$ was further reduced to 24.6 F cm^{-3} (Figure S7b in Supporting Information). The galvanostatic charge/discharge curves of CNT_1-RGO_4 WSSs with different device lengths are given in Figure 4c as well as in Figure S7a,b. At the same

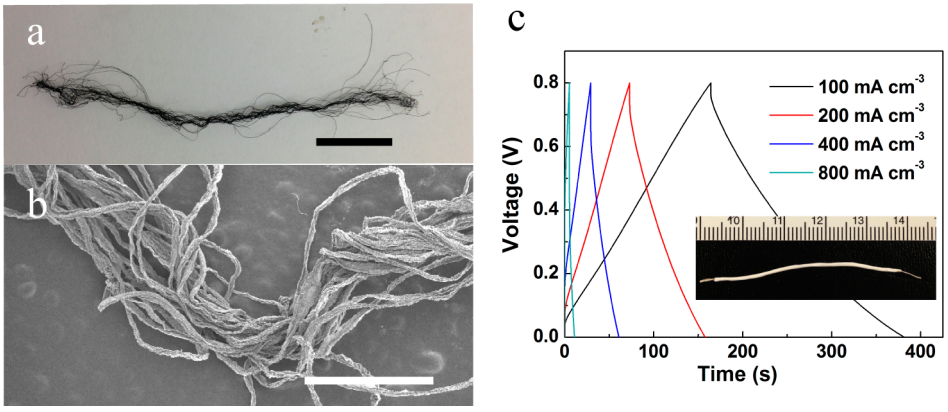

Figure 5. (a) Photograph and (b) SEM of a bundle of CNT_1-RGO_4 fibers; (c) Galvanostatic charge−discharge curves of a 4 cm WSS made from fiber-bundle electrodes. The inset in (c) is the photograph of the WSS wrapped by polytetrafluoroethylene film. Scale bars: 1 cm (a), 1 mm (b).

volumetric current density, the shorter device had a longer discharging time and a smaller voltage drop (V_{IR}) at the beginning of the discharge. The internal resistances calculated from $R_{WSS} = V_{IR}/2I_R$ at the same discharge current ($I_R = 1\ \mu A$) for 1, 3, and 6 cm devices were 5.0, 9.5, and 13.0 KΩ (Figure S7 in Supporting Information). Internal resistance increases with increasing device length, mainly due to increased linear resistance of the electrodes, which in turn lowers the capacitance of the devices. Ultimately, device length had a significant impact on the power and energy density of these devices (Figure 4d). The 1 cm WSS had the highest energy density, 3.4 mWh cm^{-3}, and power density, 0.7 W cm^{-3}; these values decreased to 2.8 mWh cm^{-3} and 0.08 W cm^{-3} for the 6 cm device. These results suggest that although frequently studied short CNT-RGO-based WSSs likely surpass film-based supercapacitors in volumetric capacitance or energy density,[14,15] the high linear resistances of these fibers needs to be resolved before larger-scale devices can be manufactured for practical energy storage applications.

In contrast to increase fiber length, plying many fibers together in each electrode is also a practical approach to elevate the capacitance of WSS.[32−34] Meanwhile, the parallel fibers can efficiently reduce the electrode resistance due to the shunt connection. To demonstrate this strategy, here we bundled 40 CNT_1-RGO_4 fibers into together for one electrode (Figure 5a). The SEM image in Figure 5b shows that these fibers maintain their individual morphology as given in Figure 2. The whole resistance was measured to be about 60 Ω cm^{-1}, much smaller than that of single fiber (∼1.1 KΩ cm^{-1}). A 4 cm WSS was assembled from this type of fiber bundles (inset in Figure 5c), presenting a $C_{WSS,L}$ of 10.2 mF cm^{-1} and R_{WSS} of 200 Ω at a charging and discharging current density of 100 mA cm^{-3} (Figure 5c). Therefore, increasing the number of fibers is a promising route to reduce the device resistance while elevate its linear capacitance.

CONCLUSIONS

A wet-spinning process to prepare CNT-RGO composite fibers with unfunctionalized FWNTs for the electrodes of WSSs was developed. The pristine FWNTs were dispersed in GO without preoxidation or the addition of surfactants, allowing the FWNTs to maintain their high conductivity and perfect structure. The incorporation of such FWNTs effectively enhanced the conductivity, tensile stress and strain of RGO fibers simultaneously. The WSSs assembled from the composite fibers with optimized CNT content showed large volumetric capacity, good rate capability, high stability and excellent flexibility. In addition, it is revealed that twisting many CNT-RGO fibers together to form shunt connection for each electrode could elevate linear capacitance, providing a possible route to resolve the performance degradation of device with solely increasing length due to the high linear resistance of a single fiber.

METHODS

Preparation of GO, CNT-GO, Reduced GO Fibers and CNT-GO Fibers. GO was synthesized from expanded graphite (3772, Asbury Graphite Mills USA) using concentrated H_2SO_4 and $KMnO_4$ as oxidants.[19] An aqueous GO dispersion (concentration 12 mg mL^{-1}) was used as a precursor to fabricate GO fibers by a Petri-dish wet-spinning method, in which GO was injected from a stainless steel needle (inside diameter: ∼100 μm) into a chitosan/acetic acid coagulation bath (3 g of chitosan and 10 mL of acetic acid dissolved in 500 mL of deionized water) by syringe pump at an injection rate of 1 mL min^{-1}. The as-spun GO fibers were washed with concentrated HCl solution and deionized water sequentially and finally dried in ambient conditions. To prepare CNT-GO composite fibers, pure FWNTs with 3−5 walls, synthesized and purified as described in our previous work,[22] were first dispersed in water by probe ultrasonication (Sonics Vibracell VC 750) for 20 min. Then FWNTs were mixed and dispersed in GO solution in a preset CNT/GO weight ratio.

The CNT-GO fibers were spun from the composite solutions using the same method as for GO fibers and were denoted as CNT_1-RGO_8, CNT_1-RGO_6, CNT_1-RGO_4, CNT_1-RGO_3, and CNT_1-RGO_2 according to the CNT/GO weight ratio from 1:8 to 1:2. The as-prepared GO and CNT-GO fibers were reduced in 50 wt % hydroiodic acid at 80 °C for 5 h, and the reduced fibers were denoted as RGO and CNT-RGO fibers, respectively.

Characterization. The structure and morphology of RGO and CNT-RGO fibers were characterized by SEM (SEM, FEI XL30). The mechanical properties of the fibers were studied using a TA Instruments RSA III microstrain analyzer. GO and GO–CNT solutions were sealed in capillary tubes for observing their dispersion state and birefringence by polarized optical microscopy (Zeiss Axio Imager) operated in transmission mode. The conductivity of RGO and CNT-RGO fibers were measured on a Keithley multimeter.

Electrochemical Measurement of Individual Electrode. Electrochemical characterizations were carried out on a Biologic SP300 instrument. CV and EIS for each fiber were taken using a three-electrode configuration in 1 M H_2SO_4 electrolyte. A saturated calomel electrode (SCE) and a platinum wire served as reference and counter electrodes, respectively.

Preparation and Performance Characterization of All-Solid-State Two-Ply WSSs. Two reduced fibers were immersed in PVA-H_3PO_4 electrolyte (10 g of PVA and 10 g of H_3PO_4 dissolved in 100 mL of deionized water) for 12 h. Then fibers were stuck together with preset overlap lengths (effective lengths) after drying in air for 1 h. The reserved electrode heads were connected to metal wires by Ag paste for the following electrochemical tests. The performance of these assembled devices was examined by CV and galvanostatic charge/discharge methods.

Conflict of Interest: The authors declare no competing financial interest.

Acknowledgment. This work is in-part supported by grants from NSF (EECS-1344745) and NSF (CHE-1213469). The authors also acknowledge the support from Duke University SMIF (Shared Materials Instrumentation Facilities). Y.M. acknowledges support from China Scholarship Council for a one-year fellowship that enabled his visit to Duke University. X.Z. is also supported by Paul M. Gross fellowship from Department of Chemistry, Duke University

Supporting Information Available: SEM characterization of GO sheets; Characterization of GO and CNT-GO liquid crystal phase; Spinnability test; Mechanical properties; Surface characterization of the reduced fibers; Electrochemical properties measured in three-electrodes configuration; Effect of device length on supercapacitor performance. This material is available free of charge *via* the Internet at http://pubs.acs.org.

REFERENCES AND NOTES

1. Gogotsi, Y. Materials Science: Energy Storage Wrapped Up. *Nature* **2014**, *509*, 568–570.
2. Jost, K.; Dion, G.; Gogotsi, Y. Textile Energy Storage in Perspective. *J. Mater. Chem. A* **2014**, *2*, 10776–10787.
3. Lima, M. D.; Fang, S. L.; Lepró, X.; Lewis, C.; Ovalle-Robles, R.; Carretero-González, J.; Castillo-Martínez, E.; Kozlov, M. E.; Oh, J. Y.; Rawat, N.; *et al.* Biscrolling Nanotube Sheets and Functional Guests into Yarns. *Science* **2011**, *331*, 51–55.
4. Ren, J.; Bai, W. Y.; Guan, G. Z.; Zhang, Y.; Peng, H. S. Flexible and Weaveable Capacitor Wire Based on a Carbon Nanocomposite Fiber. *Adv. Mater.* **2013**, *25*, 5965–5970.
5. Chen, X. L.; Qiu, L. B.; Ren, J.; Guan, G. Z.; Lin, H. J.; Zhang, Z. T.; Chen, P. N.; Wang, Y. G.; Peng, H. S. Novel Electric Double-Layer Capacitor with a Coaxial Fiber Structure. *Adv. Mater.* **2013**, *25*, 6436–6441.
6. Lee, J. A.; Shin, M. K.; Kim, S. H.; Cho, H. U.; Spinks, G. M.; Wallace, G. G.; Lima, M. D.; Lepró, X.; Kozlov, M. E.; Baughman, R. H.; *et al.* Ultrafast Charge and Discharge Biscrolled Yarn Supercapacitors for Textiles and Microdevices. *Nat. Commun.* **2013**, *4*, 1970.
7. Meng, Y. N.; Zhao, Y.; Hu, C. G.; Cheng, H. H.; Hu, Y.; Zhang, Z. P.; Shi, G. Q.; Qu, L. T. All-Graphene Core-Sheath Microfibers for All-Solid-State, Stretchable Fibriform Supercapacitors and Wearable Electronic Textiles. *Adv. Mater.* **2013**, *25*, 2326–2331.
8. Li, Y. R.; Sheng, K. X.; Yuan, W. J.; Shi, G. Q. A High-Performance Flexible Fibre-Shaped Electrochemical Capacitor Based on Electrochemically Reduced Graphene Oxide. *Chem. Commun.* **2013**, *49*, 291–293.
9. Cheng, H. H.; Dong, Z. L.; Hu, C. G.; Zhao, Y.; Hu, Y.; Qu, L. T.; Chen, N.; Dai, L. M. Textile Electrodes Woven by Carbon Nanotube–Graphene Hybrid Fibers for Flexible Electrochemical Capacitors. *Nanoscale* **2013**, *5*, 3428–3434.
10. Xu, P.; Gu, T. L.; Cao, Z. Y.; Wei, B. Q.; Yu, J. Y.; Li, F. X.; Byun, J. H.; Lu, W. B.; Li, Q. W.; Chou, T. W. Carbon Nanotube Fiber Based Stretchable Wire-Shaped Supercapacitors. *Adv. Energy Mater.* **2014**, *4*, 1300759.
11. Zhang, D. H.; Miao, M. H.; Niu, H. T.; Wei, Z. X. Coaxial Fiber Supercapacitor Using All-Carbon Material Electrodes. *ACS Nano* **2014**, *8*, 4571–4579.
12. Choi, C. S.; Lee, J. A.; Choi, A. Y.; Kim, Y. T.; Lepró, X.; Lima, M. D.; Baughman, B. H.; Kim, S. J. Flexible Supercapacitor Made of Carbon Nanotube Yarn with Internal Pores. *Adv. Mater.* **2014**, *26*, 2059–2065.
13. Meng, Q. H.; Wu, H. P.; Meng, Y. N.; Xie, K.; Wei, Z. X.; Guo, Z. X. High-Performance All-Carbon Yarn Micro-Supercapacitor for an Integrated Energy System. *Adv. Mater.* **2014**, *26*, 4100–4106.
14. Kou, L.; Huang, T. Q.; Zheng, B. N.; Han, Y.; Zhao, X. L.; Gopalsamy, K.; Sun, H. Y.; Gao, C. Coaxial Wet-Spun Yarn Supercapacitors for High-Energy Density and Safe Wearable Electronics. *Nat. Commun.* **2014**, *5*, 3754.
15. Yu, D. S.; Goh, K. L.; Wang, H.; Wei, L.; Jiang, W. C.; Zhang, Q.; Dai, L. M.; Chen, Y. Scalable Synthesis of Hierarchically Structured Carbon Nanotube–Graphene Fibres for Capacitive Energy Storage. *Nat. Nanotechnol.* **2014**, *9*, 555–562.
16. Beidaghi, M.; Wang, C. L. Micro-Supercapacitors Based on Interdigital Electrodes of Reduced Graphene Oxide and Carbon Nanotube Composites with Ultrahigh Power Handling Performance. *Adv. Funct. Mater.* **2012**, *22*, 4501–4510.
17. Ericson, L. M.; Fan, H.; Peng, H. Q.; Davis, V. A.; Zhou, W.; Sulpizio, J.; Wang, Y. H.; Booker, R.; Vavro, J.; Guthy, C.; *et al.* Macroscopic, Neat, Single-Walled Carbon Nanotube Fibers. *Science* **2004**, *305*, 1447–1450.
18. Behabtu, N.; Young, C. C.; Tsentalovich, D. E.; Kleinerman, O.; Wang, X.; Ma, A. W. K.; Bengio, E. A.; ter Waarbeek, R. F.; de Jong, J. J.; Hoogerwerf, R. E.; *et al.* Strong, Light, Multifunctional Fibers of Carbon Nanotubes with Ultrahigh Conductivity. *Science* **2013**, *339*, 182–186.
19. Zhang, M.; Atkinson, K. R.; Baughman, R. H. Multifunctional Carbon Nanotube Yarns by Downsizing an Ancient Technology. *Science* **2004**, *306*, 1358–1361.
20. Xu, Z.; Gao, C. Graphene Chiral Liquid Crystals and Macroscopic Assembled Fibres. *Nat. Commun.* **2011**, *2*, 571.
21. Jalili, R.; Aboutalebi, S. H.; Esrafilzadeh, D.; Shepherd, R. L.; Chen, J.; Aminorroaya-Yamini, S.; Konstantinov, K.; Minett, A. I.; Razal, J. M.; Wallace, G. G. Scalable One-Step Wet-Spinning of Graphene Fibers and Yarns from Liquid Crystalline Dispersions of Graphene Oxide: Towards Multifunctional Textiles. *Adv. Funct. Mater.* **2013**, *23*, 5345–5354.
22. Xiang, C. S.; Young, C. C.; Wang, X.; Yan, Z.; Hwang, C. C.; Cerioti, G.; Lin, J.; Kono, J.; Pasquali, M.; Tour, J. M. Large Flake Graphene Oxide Fibers with Unconventional 100% Knot Efficiency and Highly Aligned Small Flake Graphene Oxide Fibers. *Adv. Mater.* **2013**, *25*, 4592–4597.
23. Lu, W. B.; Zu, M.; Byun, J. H.; Kim, B. S.; Chou, T. W. State of the Art of Carbon Nanotube Fibers: Opportunities and Challenges. *Adv. Mater.* **2012**, *24*, 1805–1833.
24. Cheng, Y. W.; Lu, S. T.; Zhang, H. B.; Varanasi, C. V.; Liu, J. Synergistic Effects from Graphene and Carbon Nanotubes Enable Flexible and Robust Electrodes for High-Performance Supercapacitors. *Nano Lett.* **2012**, *12*, 4206–4211.
25. Du, J. H.; Pei, S. F.; Ma, L. P.; Cheng, H. M. Carbon Nanotube- and Graphene-Based Transparent Conductive Films for Optoelectronic Devices. *Adv. Mater.* **2014**, *26*, 1958–1991.

26. Cheng, Y. W.; Zhang, H. B.; Lu, S. T.; Varanasi, C. V.; Liu, J. Flexible Asymmetric Supercapacitors with High Energy and High Power Density in Aqueous Electrolytes. *Nanoscale* **2013**, *5*, 1067–1073.
27. Shin, M. K.; Lee, B.; Kim, S. H.; Lee, J. A.; Spinks, G. M.; Gambhir, S.; Wallace, G. G.; Kozlov, M. E.; Baughman, R. H.; Kim, S. J. Synergistic Toughening of Composite Fibres by Self-Alignment of Reduced Graphene Oxide and Carbon Nanotubes. *Nat. Commun.* **2012**, *3*, 650.
28. Qiu, L.; Yang, X. W.; Gou, X. L.; Yang, W. R.; Ma, Z. F.; Wallace, G. G.; Li, D. Dispersing Carbon Nanotubes with Graphene Oxide in Water and Synergistic Effects between Graphene Derivatives. *Chem.—Eur. J.* **2010**, *16*, 10653–10658.
29. Jalili, R.; Aboutalebi, S. H.; Esrafilzadeh, D.; Konstantinov, K.; Moulton, S. E.; Razal, J. M.; Wallace, G. G. Organic Solvent-Based Graphene Oxide Liquid Crystals: A Facile Route toward the Next Generation of Self-Assembled Layer-by-Layer Multifunctional 3D Architectures. *ACS Nano* **2013**, *7*, 3981–3990.
30. Hou, Y.; Tang, J.; Zhang, H. B.; Qian, C.; Feng, Y. Y.; Liu, J. Functionalized Few-Walled Carbon Nanotubes for Mechanical Reinforcement of Polymeric Composites. *ACS Nano* **2009**, *3*, 1057–1062.
31. Xiao, X.; Li, T. Q.; Yang, P. H.; Gao, Y.; Jin, H. Y.; Ni, W. J.; Zhan, W. H.; Zhang, X. H.; Cao, Y. Z.; Zhong, J. W.; *et al.* Fiber-Based All-Solid-State Flexible Supercapacitors for Self-Powered Systems. *ACS Nano* **2012**, *6*, 9200–9206.
32. Aboutalebi, S. H.; Jalili, R.; Esrafilzadeh, D.; Salari, M.; Gholamvand, Z.; Yamini, S. A.; Konstantinov, K.; Shepherd, R. L.; Chen, J.; Moulton, S. E. High-Performance Multifunctional Graphene Yarns: Toward Wearable All-Carbon Energy Storage Textiles. *ACS Nano* **2014**, *8*, 2456–2466.
33. Carretero-González, J.; Castillo-Martínez, E.; Dias-Lima, M.; Acik, M.; Rogers, D. M.; Sovich, J.; Haines, C. S.; Lepró, X.; Kozlov, M.; Zhakidov, A.; *et al.* Oriented Graphene Nanoribbon Yarn and Sheet from Aligned Multi-Walled Carbon Nanotube Sheets. *Adv. Mater.* **2012**, *24*, 5695–5710.
34. Jost, K.; Durkin, D. P.; Haverhals, L. M.; Brown, E. K.; Langenstein, M.; De Long, H. C.; Trulove, P. C.; Gogotsi, Y.; Dion, G. Natural Fiber Welded Electrode Yarns for Knittable Textile Supercapacitors. *Adv. Energy Mater.* **2014**, 10.1002/aenm.201401286.